J. CHEM. SOC. FARADAY TRANS., 1992, 88(22), 3287–3293

Highly Excited Vibrational States of the KCN Molecule

James R. Henderson, Hoanh A. Lam and Jonathan Tennyson
Department of Physics and Astronomy, University College London, London, WC1E 6BT UK

Vibrational ($J = 0$) states for the KCN molecule are calculated in Jacobi coordinates, employing a discrete variable representation (DVR) for the angular internal coordinate. The power of the DVR method is once again illustrated in that some 800 vibrational ($J = 0$) states are converged for a two-dimensional potential-energy surface. The energy region studied is that where the classical dynamics of the system are known to be chaotic. Most of the states are found to be irregular, although there are classes which appear to be regular and can be assigned effective quantum numbers corresponding to excitation in particular 'separable' modes of the system. Phenomenological aspects of the wavefunctions are discovered *via* graphical analysis, in particular many linearly localised states are identified where the potential-energy surface actually has a saddle point. The statistical behaviour of the level spacings is also investigated. Comparison with a similar study on LiCN (J. R. Henderson and J. Tennyson, *Mol. Phys.*, 1990, **69**, 639) is made.

In recent years experimental advances have initiated interest in the high-lying rotation–vibration states of small molecular systems. The problems involved in the rather demanding theoretical investigations have been alleviated somewhat by the recent introduction of novel techniques. A most useful method for very high-lying states is the discrete variable representation (DVR) originally proposed by Harris, Engerholm and Gwinn.[1] The DVR has been extensively developed by Bačić and Light,[2] and has seen further development and use by Tennyson, Henderson and co-workers.[3–6] The method has proved to be very useful in dealing with small molecular systems which can execute highly anharmonic and large amplitude motions, and which may have a potential-energy surface with more than one minimum. Such systems are usually regarded as being 'floppy'. The alkali-metal cyanides LiCN, NaCN and KCN are known to be of this type.

The dynamics of KCN are known from both the liquid[7] and crystalline[8,9] phases to be particularly interesting and unusual. This is because of the facile transition between the CN group being rigid and undergoing free rotation.

In the gas phase, KCN is to our knowledge unique in that classical calculations predict the onset of classical chaos below the quantum ground state of the system.[10] These calculations were also unusual in that the coupling between the K—CN bending and stretching modes was so strong that no quasiperiodic trajectories were found above the classical transition to chaos.[10,11] This behaviour should be contrasted with that of LiCN in which the Li—CN bend and stretch show much weaker coupling. In this case, the transition to classical chaos is at much higher energy and quasiperiodic trajectories can be found all the way to dissociation.[12] This behaviour is also reflected in the quantal states of this system.[3,12] Conversely, limited quantal calculations on RbCN suggest that it will display behaviour similar to that of KCN.[13]

In the gas phase, the observed spectrum of KCN has been understood only in the microwave region.[14,15] Initial studies concluded that the KCN system has a linear equilibrium geometry[14] as in LiNC and HCN, although now it is known to have a more or less T-shaped structure.[15]

Theoretical investigations on the rotation–vibration behaviour of the KCN molecule have been made by several workers,[10,16–18] but only at low energies, encompassing the first 35 states. The main reason for this is that the classical description for this system predicts a highly chaotic behaviour at very low energy indeed, and it is then usual for the corresponding quantum studies to prove difficult.

The main aim of this study is to provide further details of the interesting dynamics of the KCN system. Comparisons are made with our study of the LiNC–LiCN system.[3] KCN and LiCN are distinctly different because their equilibrium geometries are not the same (LiCN and LiNC are both linear minima on the potential), and, as noted above, the angular–radial coupling in KCN is very much stronger than in LiCN. The difference in mass between the potassium and the lithium suggests investigation into their relative (semi-)classical descriptions.

The following section gives a description of the potential-energy surface used, the calculations performed and an account of the method. The Discussion section presents our results as tabulations of energies and contour plots of various wavefunctions. The final sections then give a discussion of the interesting and phenomenological aspects of the results and conclusions.

Calculations and Results

The potential-energy surface used in this work is that due to Wormer and Tennyson,[19] and is shown in the form of a contour plot in Fig. 1. This potential was calculated at the SCF level for a fixed value of the CN bond length of 2.186 a_0.† The SCF calculations used an extended basis of 98 GTOs: (11s,6p,2d/6s,3p,2d) on C and N, and (20s,15p,1s/11s, 9p,1d). While vibrational frequencies are not usually represented accurately by the SCF approximation, this model is appropriate for the highly ionic KCN molecule, where the interaction is between closed-shell CN^- and K^+ fragments. As can be seen, this potential predicts the T-shaped minimum, in reasonable agreement with experiment.[14]

The calculations presented here were made in 'scattering' or 'Jacobi' coordinates. These coordinates are given by r_{CN}, fixed at 2.186 a_0, R, the distance of K to the CN centre of mass, and θ, the angle between r_{CN} and R. Linear KNC will then be located at 180° and linear KCN at 0°. It can be seen from the potential-surface plot that the equilibrium configuration is given by $\theta \approx 105°$ and $R \sim 5\ a_0$, with saddle points to either side at the linear configuration.

It would be well within the capabilities of our method to include the motion of the CN bond; however, there is no full three-dimensional potential available for this system. This is not surprising since any electronic structure calculation

† $1\ a_0 \approx 5.291\,77 \times 10^{-11}$ m.

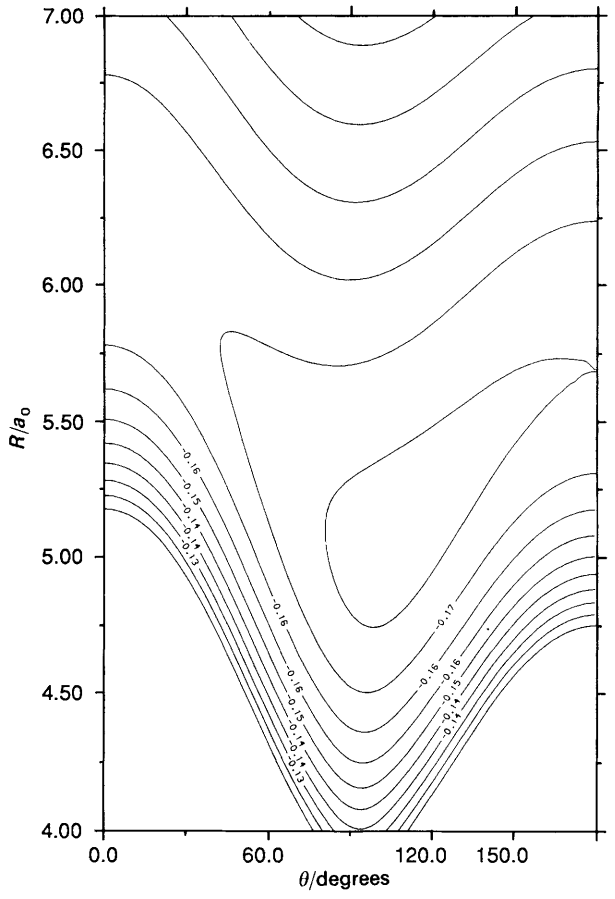

Fig. 1 Contour plot of the potential-energy surface for KCN. The vertical axis represents R, the K–CN centre of mass distance, and the horizontal axis represents the angular coordinate θ. Note that the potential minimum occurs approximately at $R = 5.0\ a_0$ and $\theta = 105°$ indicating that this system has a T-shaped equilibrium geometry. The contours are marked with their appropriate energies in E_h (1 $E_h \approx 4.359\,75 \times 10^{-18}$ J)

Table 1 Details of the radial basis functions used

	r_e	ω_e	D_e
TS[a]	5.13	0.001 18	0.173
this work	5.50	0.000 94	0.178

r_e, ω_e and D_e are give in au.
[a] Ref. (18).

hoping to treat the CN stretching coordinate reliably would be forced to use a level of correlation which would make the inclusion of a K atom in the calculation prohibitively expensive.

We would argue that freezing the CN bond is reasonable on physical grounds. Wormer and Tennyson[19] performed a number of calculations testing the effect on their optimized CN^- bond length of placing a K^+ ion at several geometries. They found that KCN behaved like an atom–diatom van der Waals complex in that the coupling between the 'intramolecular' CN^- coordinate and the other 'intermolecular' coordinates was weak. Furthermore, the CN^- has a high fundamental stretching frequency relative to the other modes which will act to weaken the coupling further.

In this work, the angle θ is represented in a DVR, with the remaining coordinate, R, being treated in the more conventional finite basis representation (FBR). This particular hybrid method, in conjunction with these coordinates, has proved successful on a number of other molecules, including LiCN[3] and HCN_2,[20,21] where angular–radial anisotropy is known to be high. H_3^+,[4] SiH_2^+,[22] Na_3[5] and H_2O[23] have also been studied successfully using our program DVR1D.[24]

The solution algorithm then is first, to make the angular coordinate discrete in point space, whilst solving the radial coordinate in the function space of the FBR. This means that for each discrete angle one diagonalises a one-dimensional (1D) Hamiltonian in the coordinate R. A selection criterion is then imposed and the N lowest 1D radial solutions are retained. These N eigenvectors are then used as a basis in which to couple the angular coordinate and solve the full problem. The angular DVR points were defined by making a direct transformation of the Hamiltonian from a Legendre polynomial basis based on Gaussian quadrature. The radial basis uses the Morse-type functions of Tennyson and Sutcliffe.[18] The functions are parametrised by three parameters r_e, D_e and ω_e, which were optimised variationally at the beginning of the investigations. The previous values used by Tennyson and Sutcliffe[18] were optimised to be appropriate for the low-lying levels. We took these and re-optimised them to be suitable for describing the high-lying levels, making sure that they could still give an adequate representation for the lower levels also. Both sets are shown in Table 1.

The final calculation converged the lowest 800 vibrational states for $J = 0$ to within 6 cm^{-1}. The first 400 levels are actually converged to within 0.1 cm^{-1}. This required 46 radial functions in R ($N_R = 45$ in the code), with 53 integration points and 72 DVR points in the angular coordinate θ ($N_\theta = 72$). The lowest 1800 intermediate solutions were selected, to construct the final Hamiltonian matrix, from a

Table 2 Convergence of the KCN band origins as a function of parameters used in the calculations

N_R	56	56	40	45	50	56	56	56
N_θ	62	72	90	90	90	80	80	80
E_{RAY}	13866	13866	14042	13950	13866	12613	13866	15231
L	1455	1661	1870	1870	1870	1578	1700	1800
level								
400	4494.2	4494.2	4494.2	4494.2	4494.2	4494.2	4494.2	4494.2
500	5089.2	5089.2	5089.4	5089.4	5089.4	5089.2	5089.1	5089.1
600	5646.6	5646.6	5647.4	5644.3	5643.9	5646.5	5646.0	5645.9
650	5905.7	5905.7	5908.4	5904.8	5904.3	5905.7	5904.0	5903.4
700	6162.2	6162.5	6185.3	6163.4	6157.5	6162.5	6158.5	6157.6
750	6425.1	6426.0	6448.7	6431.6	6429.1	6426.0	6411.5	6409.2
800	6701.4	6701.5	6748.8	6726.2	6717.5	6701.4	6661.4	6656.2

N_R gives the number of Morse oscillator-like functions used for the r_2 coordinate. N_θ gives the number of discrete points used in the angular coordinate, θ. E_{RAY} gives the cut-off energy for solutions of the 1D radial problem in cm^{-1} relative to the KNC minimum of the potential yielding a final Hamiltonian matrix of dimension L. All band origins are given in cm^{-1} relative to the KNC ground state. Comparison of levels below level 500 showed them all to be converged to within 0.1 cm^{-1} by the calculations presented here.

Table 3 Assignments for regular states localised about the KCN minimum

level no.	frequency/cm^{-1}	assignment ν_s	assignment ν_b	level no.	frequency/cm^{-1}	assignment ν_s	assignment ν_b
1	0.0	0	0	24	920.6	1?	8?
2	116.1	0	1	25	949.6	1?	10?
3	217.7	0	2	26	973.0	0	12
4	294.3	0	3?	27	1008.6	0	11
5	314.5	0	3	28	1017.7	0	11?
6	379.5	0	4	30	1068.1	0	13
7	420.4	0	5?	31	1082.1	2	8?
8	448.3	0	5	33	1126.6	0	12?
9	494.7	0	6	34	1139.7	0	13
10	530.2	1	6?	35	1173.6	0	13?
11	574.5	1	7	38	1235.2	1	13
13	623.6	0	7?	39	1251.6	0	14
14	661.0	0	8	40	1261.8	1	14
15	688.9	0	9	43	1329.4	0	16
17	739.2	1	9	46	1465.3	0	14
18	781.3	0	8?	54	1508.1	1	15
19	788.7	0	10	59	1606.8	1	16
20	838.6	0	10?	68	1724.3	1	16
23	892.0	2?	10?				

States are assigned by inspection of the wavefunction (see Fig. 2) quanta of the K—CN stretch, ν_s, and bend, ν_b. States for which the nodal structures are greatly distorted are denoted by '?'.

maximum of $46 \times 72 = 3312$. This selection criterion is equivalent to selecting all those solutions that lie below 38 929 cm^{-1}. Table 2 illustrates the convergence of a selection of levels as a function of the various parameters.

We find it very useful to make contour plots of the wavefunctions. The main advantage of this technique is that it immediately allows an identification of excitation in a particular mode, coordinate or direction, and hence can allow (tentative) assignment of quantum numbers. In this context, we refer to a particular state as being irregular if no approximate quantum numbers can be assigned in this way. We also choose to plot, with an outer dotted contour, the classical turning point for the particular state being plotted. It is then seen that an irregular state will, in general, fill up the whole of the coordinate space available to it. This method was used by Tennyson and Farantos for the lower-lying states of KCN,[10] and by Henderson, Tennyson and co-workers for the high-lying states of other systems.[3–6] For instance, this graphical analysis helped to confirm the existence of the quantum analogue of the so-called 'horseshoe' periodic orbit of H_3^+ predicted by classical mechanics.[4]

As the equilibrium geometry of KCN is approximately T-shaped, one may expect a number of states to exist about this equilibrium. We find *ca.* 70 such states, all lying below the higher of the two linear saddle points, of which we are able tentatively to assign *ca.* 36. These are tabulated in Table 3, with contour plots of some of them shown in Fig. 2.

Above the two saddle points the majority of the states observed in this work are irregular in nature. Fig. 3 shows a selection of these. As the KCN molecule is not linear, one may not necessarily expect to find linear bound states as

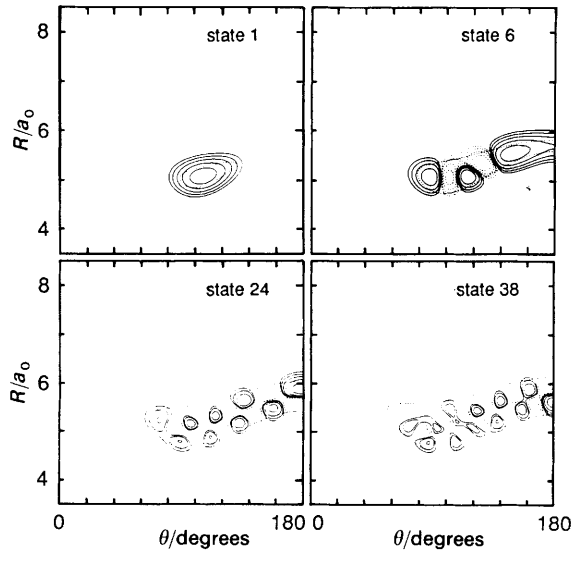

Fig. 2 Contour plots of four typical KCN states localised about the equilibrium. The axes are as in Fig. 1. Contour lines are drawn at 4, 8, 16, 32 and 64% of the maximum amplitude of the wavefunction. Those which are solid represent positive amplitude, whilst the dashed represent negative amplitude. The dashed outer contour represents the classical turning point for that particular energy

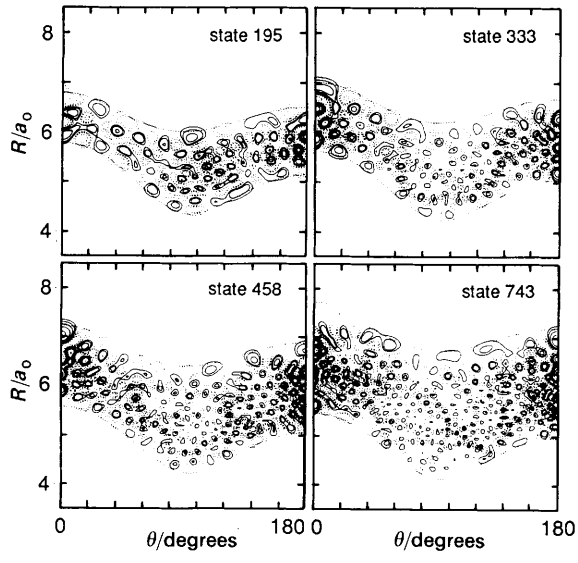

Fig. 3 Contour plots of four typical irregular, or delocalised states. Contours as in Fig. 2

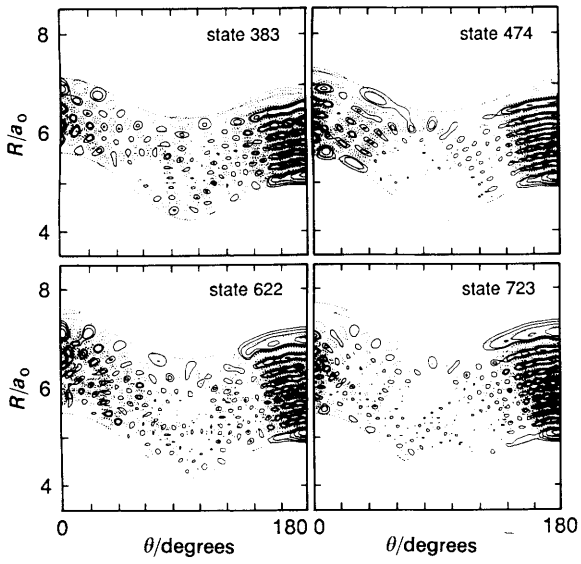

Fig. 4 Contour plots of four typical saddle-point states localised at the linear KNC geometry of the molecule; contours as in Fig. 2

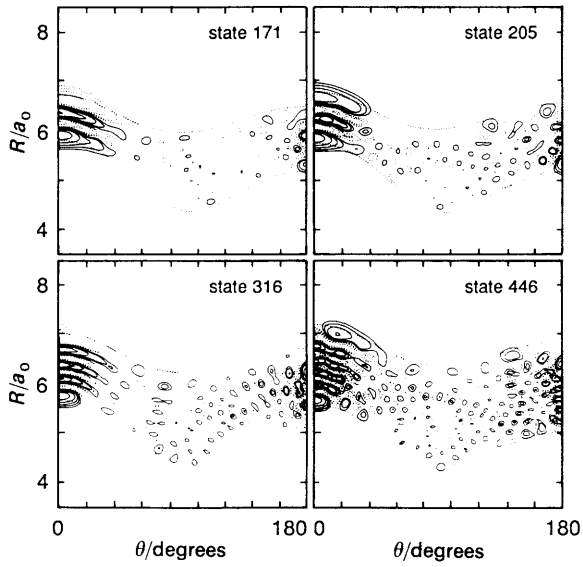

Fig. 5 Contour plots of four typical saddle-point states localised at the linear KCN geometry of the molecule; contours as in Fig. 2

these geometries are actually saddle points on the potential-energy surface. We do observe these states, however. One can actually think of them as localised isomeric transition states. Contour plots of some of these states are shown in Fig. 4 and 5. Tabulations of their energies, and approximate assignments, are given in Tables 4 and 5. We believe that this is a novel observation of a series of quantum bound states that are not localised about a potential-energy minimum.

The possibility of KCN free-rotor states, where the K^+ 'freely rotates' with high orbital angular momentum about the CN^- ion, was first discussed by Clementi *et al.*[25] Such states are found to be very pronounced in KCN, existing right across the energy range considered here. A selection of these very distinctive wavefunction patterns are shown in Fig.

Table 4 Assignments for linear KCN states

level no.	frequency/cm^{-1}	assignment v_s	assignment v_b	level no.	frequency/cm^{-1}	assignment v_s	assignment v_b
81	1920.02	0	0	361	4242.29	8	0
82	1932.85	0	2?	398	4480.23	9	0
84	1954.23	0	3?	405	4519.04	8	1
85	1968.80	0	2?	438	4725.51	10	0
86	1980.02	0	0	440	4741.70	10	0
87	1987.09	0	3?	446	4770.99	10	0
109	2237.46	1	0	449	4784.72	10	3?
110	2255.29	1	0	486	5009.69	11	2?
112	2270.54	1	0	490	5027.70	11	4?
113	2273.15	1	1?	492	5043.73	11	2?
139	2544.81	2	0	538	5302.42	12	0
140	2548.26	2	0	588	5574.05	13	3?
143	2573.34	2	1?	590	5588.34	12	2
148	2628.80	2	1	623	5764.42	13	3?
171	2834.68	3	0	626	5776.96	14	1
205	3120.28	4	0	629	5795.19	14	5?
215	3211.06	4	1?	638	5843.41	14	1
239	3392.76	5	1	642	5861.25	14	1
240	3400.67	5	0	643	5862.78	14	0
241	3405.71	5	0	684	6081.57	14	4?
258	3531.53	5	0	698	6147.54	15	6?
277	3675.79	6	0	700	6157.66	15	0
278	3677.02	6	0	702	6169.87	15	0
296	3808.03	6	1	705	6185.67	15	0
312	3911.19	7	1	709	6206.02	14	2
316	3949.64	7	0	716	6241.05	15	0
317	9955.79	7	0	728	6302.90	15?	3?
339	4102.46	7	1	736	6336.15	14	3?
349	4165.74	7	2	741	6366.39	15	2?
355	4210.98	8	0	764	6483.83	15	1
356	4215.63	8	1	788	6600.53	16	2?
360	4233.13	8	0	792	6618.08	15	3

States are assigned by inspection of the wavefunction (see Fig. 5) quanta of the K—CN stretch, v_s, and bend, v_b. States for which the nodal structures are greatly distorted are denoed by '?'.

Table 5 Assignments for linear KNC states

level no.	frequency/cm^{-1}	assignment ν_s	assignment ν_b	level no.	frequency/cm^{-1}	assignment ν_s	assignment ν_b
16	729.83	1	1?	472	4939.76	15	3?
29	1043.64	2	0	474	4946.82	15	0
36	1182.99	2	3?	476	4955.67	14	2?
47	1404.78	3	0	522	5214.97	16	1
69	1744.81	4	0	523	5221.97	16	0
92	2037.79	5	0	571	5487.34	17	0
101	2150.45	5	3	582	5549.36	13	1
118	2329.07	6	0	594	5607.68	17	2?
121	2353.47	6	0	618	5742.77	18	2?
149	2633.62	7	0	619	5746.14	18?	0
151	2650.92	7	0	620	5452.40	18?	1?
159	2725.79	7	4	622	5759.31	18	0
181	2919.89	7	0	670	6012.49	19	2
183	2934.08	8	0	672	6020.02	19	3?
184	2944.66	8	0	674	6024.23	19	3?
218	3225.39	9	0	695	6128.87	19?	2
220	3238.28	9	0	701	6168.61	19	4?
221	3243.43	9	0	708	6203.34	18	3
257	3524.07	10	0	715	6234.49	20	1?
259	3539.83	10	0	722	6276.84	20	1
298	3820.21	11	0	723	6279.69	20	0
299	3824.31	11	0	720	6311.14	18	4?
304	3861.74	11	1	734	6332.84	19	2
331	4049.00	12	0	770	6514.55	21	1
338	4100.62	12	0	775	6537.74	21	0
383	4388.53	13	0	776	6539.74	21	2
384	4390.35	13	0	775	6540.18	21	1
427	4664.12	14	3	783	6563.06	20	0
428	4670.24	14	0	793	6630.74	19	4
444	4764.43	14	0				

States are assigned by inspection of the wavefunction (see Fig. 4) quanta of the K—CN stretch, ν_s, and bend, ν_b. States for which the nodal structures are greatly distorted are denoted by '?'.

6. Free-rotor states are also found to exist with a quantum or two of stretching excitation. Their assignments and energies are given in Table 6.

Fig. 7 shows a family of states exhibiting a totally unpredicted type of state, not observed in the LiCN study.[3] This will be discussed in the next section.

A useful technique for analysing quantal energy levels whose classical analogue is chaotic is the plotting of nearest-neighbour level spacing distributions. It is said that for a selection of levels that behave regularly, the nearest neighbour spacings will tend to a Poisson distribution,[26] and for irregular levels to a Wigner distribution.[27] Fig. 8 shows four histograms, one for each equal window on the 800-state range. As can be seen, the general trend is increasingly Wigner-like as the energy increases.

Discussion

A large amount of qualitative information is obtained from the graphical analysis, in particular the nodal structure of the wavefunctions. For the first time, we have been able to inves-

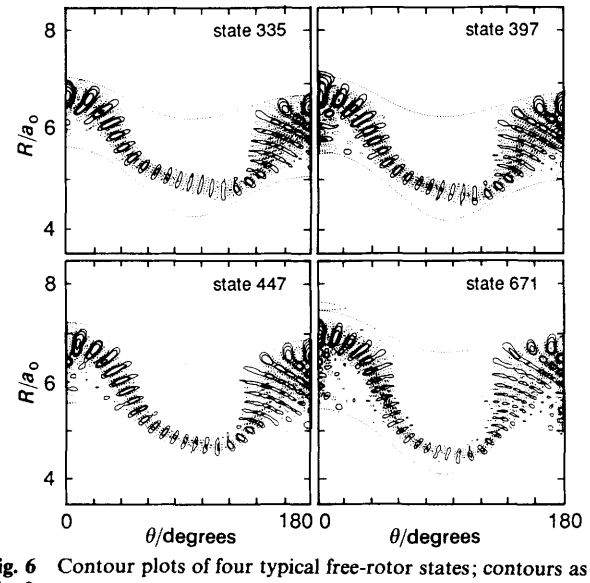

Fig. 6 Contour plots of four typical free-rotor states; contours as in Fig. 2

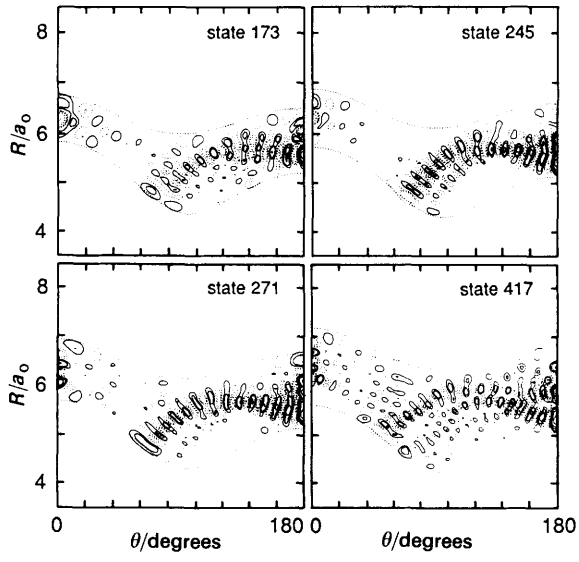

Fig. 7 Contour plots of four typical 'hingeing' states; contours as in Fig. 2

Table 6 Assignments for the free-rotor states

level no.	frequency/cm^{-1}	assignment v_s	assignment v_b	level no.	frequency/cm^{-1}	assignment v_s	assignment v_b
80	1903.83	0	19	397	4473.62	0	52
88	2005.22	1	22	409	4546.56	0	50
96	2094.09	0	22	413	4575.02	0	53
117	2316.10	0	26	423	4643.27	1	48?
120	2341.12	0	26	430	4675.29	0	54
150	2645.29	0	32?	441	4745.26	3?	54?
160	2732.33	0	32	447	4776.96	0	55
161	3747.26	0	30	463	4878.48	0	56
170	2818.69	0	32	482	4981.76	0?	57
177	2886.87	1	31?	495	5058.34	2?	54
199	3070.39	1	34	499	5084.71	0	58
210	3152.89	1	35?	516	5185.58	0	59
231	3326.46	1	37?	534	5287.50	0	54
250	3470.36	0	41	536	5290.88	0	60
265	3584.39	1	41?	551	5277.87	4?	60?
268	3603.19	0	41	554	5391.62	0	61
280	3694.47	0	42?	573	5495.70	0	62
293	3788.88	0	45	593	5599.67	0	63
307	3883.01	0	46	605	5670.37	0	58
318	3962.92	0	45	612	5703.52	2	64
319	3963.50	0	47	625	5776.22	2	64
332	4055.18	0	44	632	5807.72	0	65
335	4076.66	0	48	651	5907.99	0	66
344	4132.74	0	48	671	6015.93	0	67
347	4153.32	1	46	691	6117.20	0	68
351	4174.89	0	49	713	6224.15	0	69
365	4273.07	0	50	732	6325.25	3?	69?
377	4347.78	0	50?	754	6431.39	0	70?
379	4371.68	0	51	773	6533.99	0	70?
380	3473.11	0	51	789	6604.35	2	70
393	6680.23	1	50?	799	6649.08	1	73

States are assigned by inspection of the wavefunction (see Fig. 6) quanta of the K—CN stretch, v_s, and bend, v_b. States for which the nodal structures are greatly distorted are denoted by '?'.

tigate the behaviour of this system above the two saddle points at linearity.

Table 7 shows previously calculated (performed in FBR) levels of KCN compared with the low-lying ones of this study. Note that the previously calculated levels all lie below the two saddle points. This illustrates nicely the fact that FBR-based methods have been adequate in the past for dealing with these fairly low-energy, mode-localised motions but that the DVR now allows one to investigate the more delocalised behaviour at very much higher energies where the system may be classically chaotic or new types of quasi-periodic motion may arise.

Families of regular states are identified which are assignable in terms of zeroth-order Hamiltonians in various modes, some of which are also observed in the LiCN molecule.[3] Note that the number of 'localised equilibrium' states that are unassignable is rather large compared to that for LiCN; this could be anticipated because of the unusually low onset of classical chaos in KCN combined with the strong mode coupling.[10] In fact we note that these 'harmonic normal mode' states centred about equilibrium do not exist above state 68, whereas in LiCN–LiNC they appear at very high energies, and are almost certainly stable right the way to dissociation.[12] Furthermore, in KCN these states seem to be dominated by bending motions, whilst in LiCN the bends

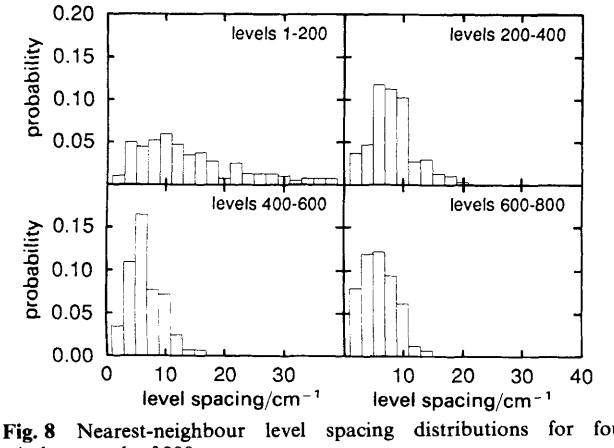

Fig. 8 Nearest-neighbour level spacing distributions for four windows, each of 200 states

Table 7 Comparison of some of the energies computed in this study with those of previous studies

state	this work	ref. (16)	ref. (17)	ref. (11)
2	116.1	116.1	116.1	—
3	217.7	217.7	217.8	—
4	294.3	294.3	294.3	—
5	314.5	314.6	314.6	314.6
6	379.5	380.0	379.6	—
7	420.4	421.2	420.5	—
8	448.3	451.8	448.4	—
9	494.7	499.7	494.9	—
10	530.2	533.4	530.4	530.2
15	688.9	—	—	688.9
20	838.6	—	—	838.6
25	949.6	—	—	949.6
30	1067.7	—	—	1067.7
35	1173.6	—	—	1173.9

Energies are given relative to the ground state which is −38 861.4 cm^{-1}.

become 'damped' at fairly low energy and very highly excited stretches predominate.

The free-rotor states are found once again to have absences in their assignments. If one plots the energy of the free rotor against $l(l + 1)$ (where l is the approximate assignment) then the result ought be approximately a straight line of gradient B, where B is the rotational constant for that motion. We find a disagreement by a factor of 2 between our gradient and an approximate 'by hand' value for B.[28] In contrast, we have found agreement to within 10% for LiCN.[28] In both molecules, the free-rotor paths do not appear necessarily to bear the same structure. In particular, it seems that the free-rotor orbits for KCN may actually be more affected by the potential-energy barrier, whereas the LiCN orbits tend to prefer to stay to the minimum-energy path. Classical trajectory calculations would be of use here.

The existence of the 'transition states', for each of the linear geometries, is somewhat surprising and rather interesting. One could say that these states are actually linear, metastable isomers of KCN. Classically, one could envisage a stability on a potential-energy local maximum so long as the motion is precisely normal to the tangent at that point. A recent study by Gomez Llorente *et al.*[29] has investigated similar behaviour. Their classical and quantum studies on the LiCN system have lead them to discuss these states as saddle-point resonances. We note that a similar, but mechanically different, phenmenon referred to as 'vibrational bonding' has been discussed by Pollak.[30]

Those plots presented in Fig. 7 represent a fascinating set of a few bound states which we shall refer to as 'hinge' motions. This can be viewed as a highly excited rotation of the K^+ about the CN^- ion, 'centred' at the N-end of the ion. It can be seen that this is not a full rotation as in the free-rotor states, but rather it is a restricted rotor and 'bounces' back from the repulsive wall at somewhere between $\theta = 60$ and 80°. So these states could actually be regarded as highly excited bending states of a quasilinear molecule, and indeed that quasilinear molecule could well be represented by the saddle-point resonances discussed above. This idea of a restricted rotor–highly excited bend against a potential wall has also been considered by Rohlfing in studies on the C_3 molecule.[31] Note that states 245 and 417 also seem to have a degree of stretching excitation.

Conclusions

We have been able to compute 800 accurate bound states for the non-linear 2D KCN system. In comparison to LiCN, some remarkable, rather unexpected, differences in the nature and dynamics of the vibrational states exist. Also it appears, in accordance with classical predictions, that the onset of chaos is much sooner and stronger in KCN. The majority of states are certainly irregular and delocalised. The predicted regular states corresponding to model Hamiltonians were observed, along with the identification of two more interesting types of motion. The identification of the hingeing motion and the transition states suggests that classical investigations would be of use.

As yet, no classical studies have discovered any periodic orbits for this system, unlike LiCN. We feel that this study may encourage and assist further calculations.

We thank Florentino Borondo and Rosa Benito for helpful discussions. J.R.H. acknowledges the SERC for a Fellowship.

References

1 D. O. Harris, G. O. Engerholm and W. Gwinn, *J. Chem. Phys.*, 1965, **43**, 1515.
2 Z. Bačić and J. C. Light, *Annu. Rev. Phys. Chem.*, 1989, **40**, 469.
3 J. R. Henderson and J. Tennyson, *Mol. Phys.*, 1989, **69**, 639.
4 J. Tennyson and J. R. Henderson, *J. Chem. Phys.*, 1989, **91**, 3815.
5 J. R. Henderson, S. Miller and J. Tennyson, *J. Chem. Soc., Faraday Trans.*, 1990, **86**, 1963.
6 J. R. Henderson and J. Tennyson, *Chem. Phys. Lett.*, 1990, **173**, 133.
7 S. Miller and J. H. R. Clarke, *J. Chem. Soc., Faraday Trans. 2*, 1974, **74**, 160.
8 H. T. Stokes and R. D. Swinney, *Phys. Rev. B*, 1985, **31**, 7153.
9 P. Bourson and P. Durand, *Ferroelectrics*, 1991, **124**, 339.
10 J. Tennyson and S. C. Farantos, *Chem. Phys. Lett.*, 1984, **109**, 160.
11 S. C. Farantos and J. Tennyson, *J. Chem. Phys.*, 1985, **82**, 800.
12 J. Tennyson and S. C. Farantos, *Chem. Phys.*, 1985, **93**, 237.
13 G. Brocks, *Chem. Phys.*, 1987, **116**, 33.
14 P. Kuijpers, T. Törring and A. Dymanus, *Chem. Phys. Lett.*, 1976, **42**, 423.
15 T. Törring, J. P. Bekooy, W. L. Meerts, J. Hoeft, E. Tiemann and A. Dymanus, *J. Chem. Phys.*, 1980, **73**, 4875.
16 J. Tennyson and B. T. Sutcliffe, *Mol. Phys.*, 1982, **46**, 97.
17 J. Tennyson and A. van der Avoird, *J. Chem. Phys.*, 1982, **76**, 5107.
18 J. Tennyson and B. T. Sutcliffe, *J. Chem. Phys.*, 1982, **77**, 4061.
19 P. E. S. Wormer and J. Tennyson, *J. Chem. Phys.*, 1981, **75**, 1245.
20 Z. Bačić and J. C. Light, *J. Chem. Phys.*, 1987, **86**, 3085.
21 M. Mladenovic and Z. Bačić, *J. Chem. Phys.*, 1990, **93**, 3039.
22 C. R. Le Sueur and J. Tennyson, to be published.
23 J. A. Fernley, S. Miller and J. Tennyson, *J. Mol. Spectrosc.*, 1991, **150**, 597.
24 J. R. Henderson and J. Tennyson, *Comput. Phys. Commun.*, to be submitted.
25 E. Clementi, H. Kistenmacher and H. Popkie, *J. Chem. Phys.*, 1972, **57**, 5137.
26 M. V. Berry and M. Tabor, *Proc. R. Soc., London, Ser. A*, 1977, **356**, 375.
27 P. Pechukas, *Phys. Rev. Lett.*, 1983, **51**, 943.
28 F. Borondo and R. Benito, personal communication.
29 J. M. Gomez Llorente, F. Borondo, N. Berenguer and R. M. Benito, *Chem. Phys. Lett.*, 1992, **192**, 430.
30 E. Pollak, *Comm. At. Mol. Phys.*, 1985, **15**, 73.
31 E. A. Rohlfing, *J. Chem. Phys.*, 1989, **91**, 4531.

Paper 2/03266J; *Received* 22*nd June*, 1992